Structural Basis for Ligand Discrimination and Response Initiation in the Heme-Based Oxygen Sensor FixL[†]

Kenton R. Rodgers,* Gudrun S. Lukat-Rodgers, and Jason A. Barron

Department of Chemistry, North Dakota State University, Fargo, North Dakota 58105

Received December 29, 1995; Revised Manuscript Received April 15, 1996[⊗]

ABSTRACT: FixL is a multiple-domain bacterial O_2-sensing protein that modulates the activity of its kinase domain in response to O_2 concentration. The kinase activity is coupled, via phosphoryl transfer, to transcriptional activation by a response-regulating protein, FixJ. Heme ligation resulting in a transition from high to low spin inhibits the kinase through an, as yet, ill-defined mechanism. This report presents spectroscopic, kinetic, and thermodynamic data on various complexes of two deletion derivatives of *Rhizobium meliloti* FixL, FixLN (the heme domain) and a functional heme kinase, FixL*. Resonance Raman characterization of metFixLN and metFixL* indicates that the heme core is smaller than that observed in metmyoglobin and is indicative of a five-coordinate high-spin heme in metFixLs. Resonance Raman spectra of FixL−CO adducts reveal that the Fe−C═O unit and/or its electrostatic environment in FixL*−CO is distorted relative to that in FixLN−CO. The ^{1}H NMR spectra of the met forms further support the model of an asymmetric perturbation of the heme pocket structure associated with the presence of the kinase domain in FixL*. Observation of equivalent Fe−imidazole stretching vibrations for deoxyFixLN and deoxyFixL* (212 cm^{-1}) indicates that the source of this perturbation in the heme pocket of FixL* does not lie on the proximal side of the heme. The equivalent Fe−imidazole stretching frequencies for deoxyFixLN and FixL* indicate that the presence of the kinase domain does not alter the relative strength of the proximal Fe−imidazole bond and that the proximal imidazole ligand is weakly H-bonded, probably to a backbone carbonyl group. Kinetic and thermodynamic data for the reactions of cyanide and fluoride ions with FixL are consistent with shape selectivity due to steric and/or an anisotropic electrostatic field in the distal heme pocket being responsible for the unique reactivities (or lack thereof) of FixL with ligands, *i.e.*, O_2, CO, CN^-, F^-, N_3^-, and SCN^-. While the rate constants for binding of CN^- to metFixLN and metFixL* are an order of magnitude slower than that for metMb, the stabilities of these complexes and metMb−CN are nearly the same. Neither N_3^- nor SCN^- binds to the heme with measurable affinity. Since other ferric heme proteins form stable adducts with these ligands, the inability of FixL to form analogous complexes suggests that the ligand selectivity of this protein is rooted in insurmountable activation barriers to the binding of ligands containing more than two atoms and for ligands whose lowest-energy coordination geometries are linear. This allows the natural O_2 ligand to compete kinetically with other naturally occurring ligands that form stable complexes with unencumbered hemes. Moreover, the rate constant for binding of CN^- to the functional heme−kinase (metFixL*) is smaller than its metFixLN counterpart and the stability of metFixL*−CN is measurably lower than that of metFixLN−CN. This indicates that the contacts between the heme and kinase domains of FixL* impose more stringent geometric constraints on ligand binding than FixLN. The kinase is thus implicated in a possible mechanism for phosphate-dependent feedback control over ligand affinity of the heme.

FixL is a cytoplasmic membrane-bound O_2-sensing protein that binds O_2 reversibly (Gilles-Gonzalez et al., 1991). It occurs in nitrogen-fixing (*Rhizobium*) bacteria that enter into symbiosis with legumes. FixL, a protein histidine kinase, and FixJ, a response regulator, constitute the two-component signal transduction system that modulates the level of *nifA* and *fixK* transcription in response to changes in cellular oxygen tension (David et al., 1988; Ditta et al., 1987). The protein products of these genes, in turn, promote transcription of all other genes necessary for nitrogen fixation in legume root nodules (Batut et al., 1989; Earl et al., 1987). FixL responds to low oxygen concentrations with increased autophosphorylation activity of its kinase domain; the deoxy form of FixL is phosphorylated by ATP. The phosphorylated deoxyFixL provides a phosphoryl group to FixJ. In its phosphorylated form, FixJ is a transcriptional activator for the *nifA* and *fixK* genes (Reyrat et al., 1993). This sequence of events is illustrated in Figure 1. The deactivation of the FixL kinase domain occurs when deoxyFixL binds oxygen. OxyFixL is unable to activate FixJ. Hence, the FixL/FixJ system constitutes an oxygen-sensitive switch for control over production of the nitrogen fixation system in these bacteria.

The spin state of the heme iron in FixL has been shown to control the activity of the kinase domain (Gilles-Gonzalez et al., 1995). In its oxy state, a low-spin form for the protein, FixL does not autophosphorylate and, therefore, cannot transfer a phosphoryl group to FixJ. In deoxy FixL the iron is high-spin and the kinase domain is activated. The

[†] This research was supported by the NDSU Chemistry Department, Graduate College and College of Science and Math, and North Dakota EPSCoR (NSF 10-82177).

* Author to whom correspondence should be addressed.

[⊗] Abstract published in *Advance ACS Abstracts,* July 1, 1996.

S0006-2960(95)03085-6 CCC: $12.00

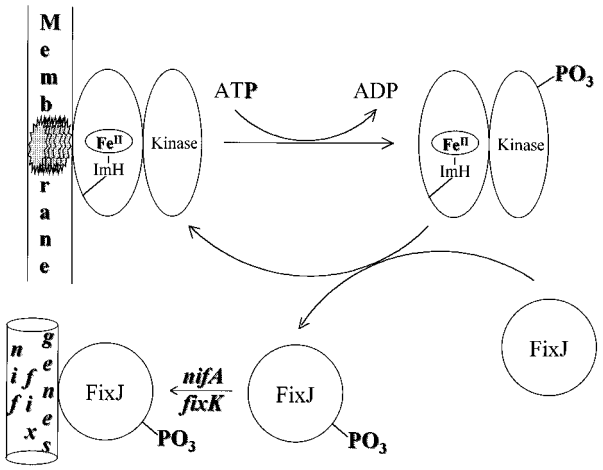

FIGURE 1: Schematic illustration of the signaling pathway through which the FixL/FixJ two-component system activates transcription of *nifA* and *fixK*. The membrane has been omitted from the phosphoFixL for clarity.

mechanism(s) involved in the transmission of the iron spin and ligation states in the heme domain to the kinase domain are not understood.

The heme in FixL does not have any known catalytic function, nor does it store or transport oxygen. Although the function of FixL is fundamentally different from that of the hemoglobins (Hb), some of its chemical and spectroscopic characteristics are strikingly similar to those of Hb (Gilles-Gonzales et al., 1991). Similarity of the UV−visible spectra of deoxy- and oxyFixL to those of the deoxy and oxy forms of myoglobin (Mb) and Hb and a recent site-directed mutagenesis study provide compelling evidence that the proximal heme ligand in FixL is the imidazole side chain of a histidine residue (His 194) (Monson et al., 1995).

FixL represents a unique opportunity to exploit the well-characterized heme chromophore to initiate and investigate the transduction of a cellular signal from its *first* step. The initial phase of this study has been to characterize the heme pocket by its spectroscopic signatures and its chemistry with small ligands. In order to avoid the inhomogeneity problems often associated with the study of membrane-bound proteins, two soluble deletion derivatives of FixL have been examined. The first is a soluble functional heme−kinase designated FixL*. This derivative contains the heme and kinase domains (residues 127−505, MW ∼42 800) (Monson et al., 1992) without the membrane anchor. The second contains only the heme domain (residues 127−260, MW ∼16 100) (Monson et al., 1992) and is designated FixLN.

Herein we present kinetic, thermodynamic, and spectroscopic data on the reaction of FixL with small ligands. These data are interpreted and analyzed in terms of the unique reactivity of the FixL heme, which they reveal. For example, the affinity of metFixL for CN^- is similar to that for metMb (horse). However, the rate constants for CN^- binding and dissociation are roughly an order of magnitude slower for metFixL than for metMb. This suggests that the nature of the heme environment is quite different from those of the well-characterized heme proteins. Differences in the NMR and resonance Raman (RR) spectroscopic signatures of metFixL and metMb are correlated with the kinetic differences to formulate a structure−function model for the heme pocket of FixL. Comparison of these data for FixLN and FixL* provides insight into the influence of the kinase domain on the heme environment. Interdomain interactions are manifested in perturbation of the heme pocket structure that result in changes in the kinetic and thermodynamic parameters for ligand binding. Resonance Raman signatures of FixL−CO and metFixL are presented and are consistent with steric crowding of the distal heme pocket that is modulated through interactions between the heme and kinase domains.

EXPERIMENTAL PROCEDURES

Expression and Purification. A soluble truncated FixL (FixL*) and the heme-containing domain of FixL (FixLN) of *Rhizobium meliloti* were overproduced in *Escherichia coli* from single plasmid constructs (pGG820 and pEM130) (Monson et al., 1992) kindly provided by Professor Donald Helinski. Both proteins were purified using published procedures (Monson et al., 1992). Protein purity was assayed via SDS−PAGE and examination of the visible spectrum in the Soret region of the spectrum. Autophosphorylation activity of purified FixL* was confirmed by anaerobic phosphorylation assays in which 4.9 μM FixL* in 20 μL of 100 mM Tris/HCl, pH 7.8, 5% glycerol, and 50 mM KCl was reduced by addition of a stock solution of sodium dithionite followed by the addition of a stock $MnCl_2$/ATP solution to yield a final concentration of 0.4 mM $MnCl_2$, 0.4 mM ATP, and 3 μCi of [γ-^{32}P]ATP. After 5 min, the reactions were stopped and analyzed via SDS−PAGE and autoradiography according to published procedures (Gilles-Gonzalez et al., 1991).

K_d Determinations and Kinetics Experiments. For protein reactions with cyanide and fluoride, both FixL* and FixLN were allowed to oxidize to their met forms at room temperature prior to use. Dissociation constants for metFixL*−CN and metFixLN−CN were determined by anaerobic titration of the respective proteins with stock, degassed cyanide solutions. Each titration point was monitored at 397 or 424 nm to ensure that the reaction mixture was at equilibrium prior to the addition of the next aliquot of cyanide solution. One to two hours was typically allowed for the reaction to reach equilibrium. If the titration was not done under anaerobic conditions, the cyanide concentration changed during the course of the equilibration time. Initially the changes in cyanide concentrations were noted for cyanide titrations of FixL* in 100 mM Tris/HCl, pH 7.8, and 5% glycerol. Similar behavior was also noted for the myoglobin cyanide titration under the same conditions. To determine if oxygen was involved in the cyanide degradation, stock solutions of sodium cyanide were prepared both aerobically and anaerobically. These stock solutions were then used in cyanide titrations of myoglobin as a test of the cyanide concentration integrity.

For kinetic measurements of CN^- binding to metFixL* and metFixLN, protein concentrations were ∼1 μM and the absorbance change at 423 or 397 nm was monitored with a spectrophotometer upon initiation of the reaction by addition of a stock cyanide solution. The reactions were carried out in a thermostatically controlled cell with stirring. Reaction conditions were varied to consider the effect of the presence of Mn^{2+}, KCl, and glycerol on the rates of cyanide binding. All the cyanide reactions were carried out under anaerobic conditions. All kinetic runs were done in triplicate at 22 °C. Measurement of the rate constant for cyanide binding

to myoglobin under conditions analogous to those used for our FixL cyanide binding studies were done in order to compare our FixL behavior to that we observed for myoglobin and for comparison to the myoglobin literature values.

The on rates for fluoride binding to the FixL proteins were measured in a manner analogous to the FixL cyanide measurements with absorbance changes monitored at 408 or 397 nm. Stock NaF solutions were prepared in 500 mM sodium phosphate, pH 7.8, and used immediately. In order to study the FixL−fluoride dissociation rate, a concentrated stock solution of the protein was treated with a 1000-fold excess of NaF. This protein fluoride mixture was then diluted into a UV−visible spectrophotometer cell containing 100 mM sodium phosphate, pH 7.8, at 22 °C. The disappearance of the FixLN−fluoride Soret was observed at 408 nm.

Titrations of FixLN and FixL* with azide and thiocyanate were attempted. These attempts were monitored via the UV−visible absorption spectrum. Sodium azide was introduced up to a 6000-fold excess over the 2 μM protein. A 13 000-fold excess of sodium thiocyanate over 2 μM protein was employed.

Circular Dichroism Experiments. A scanning CD spectrometer was used to obtain a CD spectrum of 2.7 μM FixLN in 20 mM sodium phosphate, pH 7.8, in a 1-cm path length cell. The method of Sreerama and Woody (Sreerama et al., 1993) was used to estimate the secondary structure composition of FixLN on the basis of the CD data. The same results were obtained regardless of the initial guesses for secondary structure composition, which suggests that these results represent the closest approach to a global minimum attainable with the algorithm of Sreerama and Woody.

Nuclear Magnetic Resonance Spectroscopy. Proton NMR spectra of metFixLN and metFixL* were obtained at 270 or 400 MHz using standard presaturation of the HDO signal from solvent water. Samples were concentrated and exchanged into 90 mM potassium phosphate, pD 7.8, and 10% glycerol in D_2O. Spectra were acquired at 18 °C.

Resonance Raman Spectroscopy. Resonance Raman spectra were acquired from samples in a spinning 5-mm NMR tube using the 135° backscattering geometry and *f*1 collection. Either the 406.7- or the 413.1-nm line from a Kr ion laser was used for Raman excitation, and the laser beam was focused to a line using a cylindrical lens to minimize photolysis artifacts and laser-induced sample degradation. Scattered light was passed through a holographic notch filter and a polarization scrambler and then *f*-matched to a 0.67-m single spectrograph fitted with a 110- × 110-mm grating having a groove density of 2400 grooves/mm. The Raman spectrum was detected using a 25-mm liquid N_2-cooled CCD camera under the control of a microcomputer. Protein concentrations in samples used for collection of resonance Raman data fell in the range of 5 μM−0.2 mM. DeoxyFixLs were generated under anaerobic conditions by addition of an aliquot of stock sodium dithionite solution. The corresponding heme−CO derivatives were prepared by addition of 1 atm CO to the tubes containing the deoxyFixLs.

RESULTS

Circular Dichroism Spectroscopy. Since the molecular weight of FixLN is similar to that of Mb (Antonini & Brunori, 1971) (Monson et al., 1992) and since the low-spin UV−visible spectra are very similar to those of Mb (Antonini & Brunori, 1971) (Monson et al., 1992), the circular dichroism (CD) spectrum of FixLN was obtained in order to compare its secondary structure to that of Mb. FixLN exhibits no significant sequence homology (Gilles-Gonzalez et al., 1994) with any structurally characterized proteins. Figure 2 shows the CD spectrum of oxyFixLN in 10 mM phosphate buffer at pH 7.8 and the results of the calculation to estimate its secondary structure composition. These results reveal that the secondary structure of the FixL heme domain is measurably different from that of Mb [78.0% α-helix, 10.0% turn, 12.0% disordered (Sreerama & Woody, 1993)] and of the subunits of tetrameric Hb.

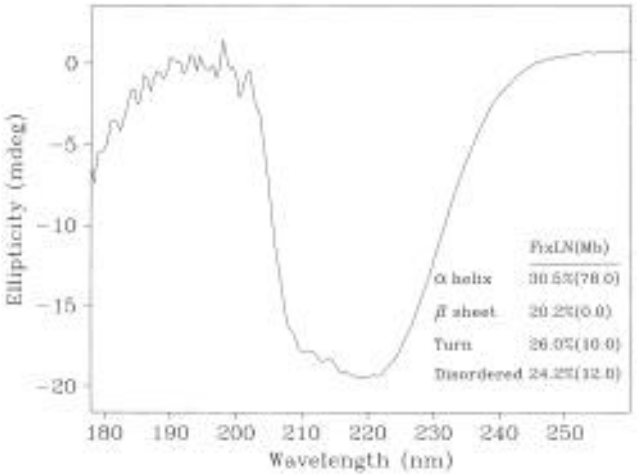

FIGURE 2: UV circular dichroism spectrum of 2.7 μM oxyFixLN in 10 mM phosphate buffer, pH 7.8. The table contains the calculated secondary structure composition for FixLN. Corresponding values for myoglobin are given in parentheses.

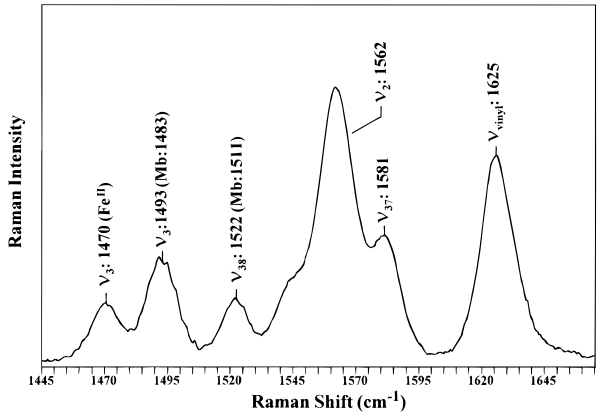

FIGURE 3: Resonance Raman spectrum of 50 μM metFixLN. The spectrum was acquired with 413.1-nm excitation and 20-mW laser power at the sample using a line focus. Band assignments are made by analogy with metMb and ferric CCP (Smulevich et al., 1996). Solution conditions are 100 mM Tris, pH 7.8, and ambient temperature. The 1470-cm^{-1} band is from ferrous heme generated by photoreduction in the laser beam. The frequencies for ν_3 and ν_{38} of aquometMb are given in parentheses. See text for discussion.

High-Frequency Resonance Raman Spectroscopy. The heme pocket structure and heme geometry of metFixLs have been probed by Soret-excited resonance Raman spectroscopy. Figure 3 shows the spectrum of metFixLN in the region of the spectrum containing vibrational modes whose frequencies are sensitive to the heme core size. These data show a marked increases in the frequencies of isolated core-size marker bands, consistent with a metFixL heme core that is

Table 1: Raman Vibrational Mode Compositions and Frequencies for metFixLN and metMb

Raman vibrational mode[a]	Raman vibrational mode composition[b]	band frequency for metFixLN[c] (cm^{-1})	band frequency for metMb[d] (cm^{-1})
ν_3	28% $\nu(C_\alpha C_{meso})$ 28% $\nu(C_\beta C_\beta)$ 12% $\nu(C_\alpha N)$	1493	1483
ν_{38}	62% $\nu(C_\beta C_\beta)$ 14% $\nu(C_\beta C_1)$[e]	1522	1511

[a] Assignments made by analogy with those for metMb and ferric CCP (Smulevich et al., 1996). [b] Compositions from the in-plane NiOEP force field (Li et al., 1990). [c] Spectra acquired using 413.1-nm excitation. [d] Hu and Spiro (submitted for publication). [e] C_1 is the carbon directly attached to the C_β carbon of a pyrrole ring.

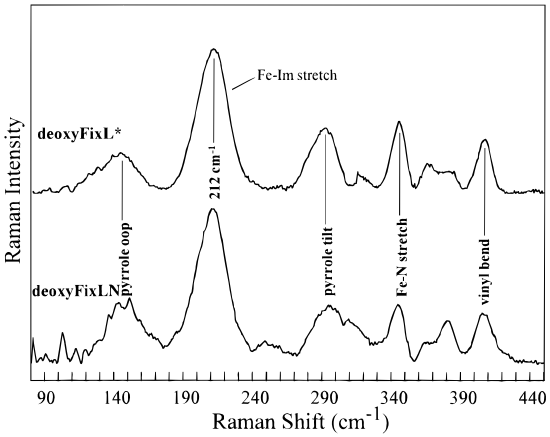

FIGURE 4: Resonance Raman spectra of 50 μM deoxyFixL* (top) and FixLN (bottom) obtained with 406.7-nm excitation and 40-mW laser power at the sample. Band assignments are made by analogy with NiOEP (Li et al., 1990) and CCP (Smulevich et al., 1996). Solution conditions are 100 mM Tris, pH 7.8, ~2 mM dithionite, and ambient temperature.

Table 2: Fe−His Stretching Frequencies in Five-Coordinate High-Spin Ferrous Heme Proteins

protein	ν_{Fe-His} (cm^{-1})	reference
sGC	204	Deinum et al. (1996)
T-state αHbA	207	Nagai and Kitagawa (1980)
FixLN	212	this work
FixL*	212	this work
R-state αHbA	218	Nagai and Kitagawa (1980)
Mb	220	Kitagawa et al. (1979)
T-state βHbA	220	Nagai and Kitagawa (1980)
R-state βHbA	224	Nagai and Kitagawa (1980)
HRP	244	Teraoka and Kitagawa (1981)

smaller than that of aquometMb. Table 1 shows the mode compositions along with their frequencies in metFixLN and aquometMb. The analogous spectrum of metFixL* is virtually identical and is not shown.

Low-Frequency Resonance Raman Spectroscopy. Figure 4 contains the Soret-excited RR spectra of deoxyFixLN and deoxyFixL*. The band at 212 cm^{-1} is assigned to the Fe−His stretching vibration by analogy with a host of other heme proteins having proximal imidazole ligands (Spiro, 1983). Figure 4 shows that the frequencies of the Fe−His stretching bands for deoxyFixLN and deoxyFixL* are indistinguishable. Table 2 shows where the ν_{Fe-His} frequencies for deoxyFixLs fall relative to the analogous vibration for a number of heme proteins.

Resonance Raman Spectroscopy of FixLN−CO and FixL−CO.* Resonance Raman spectra of heme−CO adducts can provide useful insight into the distal heme environments in heme proteins. The most intense band in Soret-excited RR spectra of porphyrin complexes is labeled ν_4 and involves primarily pyrrole N−C_α and pyrrole C_α−C_β stretching and C_α−C_{meso} bending (Li et al., 1990). Figure 5 shows ν_4 for the low-spin Fe^{II}−CO adducts of FixLN and FixL*. Note that ν_4 for FixL*−CO is shifted to lower frequency (downshifted) 2.7 cm^{-1} from that of the FixLN−CO complex. Careful inspection of Figure 5 reveals that the bandwidth of ν_4 for FixL*−CO is slightly greater than that for FixLN−CO.

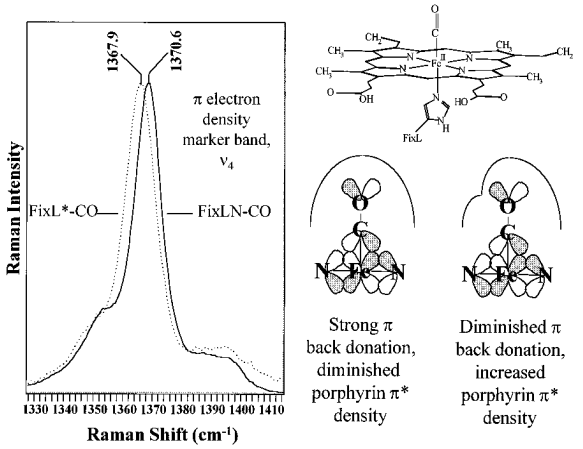

FIGURE 5: ν_4 region of the 406.7-nm excited resonance Raman spectra of FixLN−CO and FixL*−CO showing the 2.7-cm^{-1} downshift and slight broadening due to interaction between the kinase and heme domains in FixL*. Illustrations show the preferred geometry of the Fe−C═O unit and how kinase-induced asymmetry in the heme pocket might perturb π backbonding between the heme and CO.

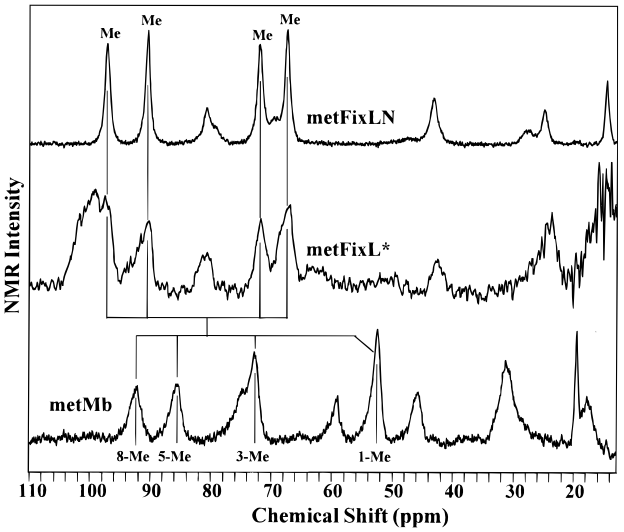

FIGURE 6: (Top) ^{1}H NMR spectrum (400 MHz) of 200 μM metFixLN, 50 mM phosphate, pD 7.8, T = 22 °C. (Middle) ^{1}H NMR (400 MHz) spectrum of 50 μM metFixL*, 50 mM phosphate, pD 7.8, T = 22 °C. (Bottom) ^{1}H NMR (270 MHz) spectrum of 500 μM metMb, 50 mM phosphate, pD 7.8, T = 22 °C. Ferric Mb spectrum is presented for comparison showing heme methyl assignments (LaMar et al., 1980). FixL heme methyl assignments are made on the basis of relative intensities, since each methyl contains three protons.

^{1}H NMR Spectroscopy of metFixLN and metFixL.* The ^{1}H NMR spectra of the five-coordinate high-spin forms of metFixLN and metFixL* are shown in Figure 6. The general features of these spectra are typical of high-spin Fe(III) hemes

Table 3: Rate and Stability Constants for Heme−Fluoride Complexes

protein	k_{on}[a,b] (M^{-1} s^{-1})	k_{off}[a] (s^{-1})	K_d[c] (M)	$\Delta G°$ [a] (kcal·mol^{-1})
metFixLN−F[e]	5.61 ± 0.47	(4.14 ± 0.06) × 10^{-2}	(7.38 ± 0.63) × 10^{-3}	−2.87
metMb−F[f]	0.53	9.4 × 10^{-3}	1.78 × 10^{-2}	−2.35
ferric HRP−F[g]	(1.8 ± 0.2) × 10^{3}	(4.5 ± 0.7) × 10^{2}	(2.5 ± 0.6) × 10^{-1}	−0.81

[a] T = 22 °C, pH 7.8, 100 mM phosphate. [b] Measured under pseudo-first-order conditions. [c] Calculated from k_{on} and k_{off}. [d] Calculated from K_d. [e] This work; reported uncertainties were obtained by propagation of the uncertainties in slopes of the log plots. [f] pH 7.95, T = 22 °C (Blank et al., 1961). [g] HRP = horseradish peroxidase, T = 25 °C, pH 7.5 (Dunford & Alberty, 1967).

Table 4: Rate and Stability Constants for Heme−Cyanide Complexes

protein	k_{on}[a,b] (M^{-1}·s^{-1})	k_{off} (s^{-1})	K_d[b] (M)	$\Delta G°$ [c] (kcal·mol^{-1})
metFixLN−CN[d,e]	32.5 ± 2.3	4.74 × 10^{-4} [f]	(1.48 ± 0.11) × 10^{-5}	−6.52
metFixLN−CN[d,g]	32.5 ± 1.6			
metFixL*−CN[d]	22.1 ± 2.2	3.98 × 10^{-4} [f]	(1.80 ± 0.03) × 10^{-5}	−6.40
metMb−CN	269 ± 15[d]	4.8 × 10^{-3} [f]	1.78 × 10^{-5} [h]	−6.41
ferric HRP−CN[f]	(7.2 ± 0.4) × 10^{4}	(2.9 ± 0.3) × 10^{-1} [f]	(3.5 ± 0.1) × 10^{-6}	

[a] Measured under pseudo-first-order conditions. [b] T = 22 °C, pH 7.8, 100 mM Tris. [c] Calculated from K_d. [d] This work; reported uncertainties were obtained by propagation of the uncertainties in slopes of the log plots. [e] Glycerol present. [f] Calculated from K_d and k_{on}. [g] Buffer was 50 mM KCl, 0.20 mM $MnCl_2$, and 5.5% glycerol. [h] Blank et al. (1961). [i] T = 25 °C, pH 8.11 (Ellis & Dunford, 1968).

(Ho, 1992; La Mar et al., 1980) and the heme methyl proton assignments indicated on the spectra were made by analogy with the spectra of the peroxidases (Lukat et al., 1989) and myoglobin (La Mar et al., 1980). The spectra of these two FixL deletion derivatives are similar except for the breadth of the resonance centered at ∼100 ppm in the metFixL* spectrum. Although all of the resonances in the metFixL* spectrum are broadened relative to their analogs in the metFixLN spectrum because of the increased molecular weight (and longer correlation time, τ_c) of metFixL* (42.8 kDa) over that of FixLN (16.1 kDa), the most downfield-shifted resonance in the metFixL* spectrum is approximately 2.5 times as broad as the other three (Figure 6). This metFixL* spectrum was obtained from a very dilute solution (∼50 μM) due to limited protein solubility. Consequently, the signal to noise ratio is somewhat small and data processing is difficult. The extensive baseline correction necessary to present the spectrum distorts the intensities to such an extent that the integrated peak intensities have little or no meaning. The spectra have been processed a number of times and the relative intensities of the most downfield-shifted peaks are not reproducible. However, regardless of the apparent intensities, the line width of the 100-ppm heme methyl resonance is always greater than the other three.

Ligand Binding to metFixLs. The dissociation constants have been measured for metFixLN−CN and metFixL*−CN by spectrophotometric titration and for metFixLN−F by determination of the association and dissociation rate constants. Thermodynamics and kinetic parameters for the reaction between metFixLN and F^- are listed in Table 3 with the corresponding data for metMb−F and HRP−F (fluoride complex of ferric horseradish peroxidase). These results show that metFixLN has slightly higher affinity for F^- than metMb [$K_{d(metMb-F)} = 2.4K_{d(metFixLN-F)}$]. Although the stabilities of these adducts differ only slightly, metFixLN's rate constant for F^- association is an order of magnitude (10.6 times) larger and that for dissociation is nearly twice (4.4 times) as large as that for metMb−F. The K_d for HRP-F is over 30 times that for the metFixL adduct. In addition to its relatively low stability, the association and dissociation rate constants for HRP−F are much larger than those for the O_2-binding proteins.

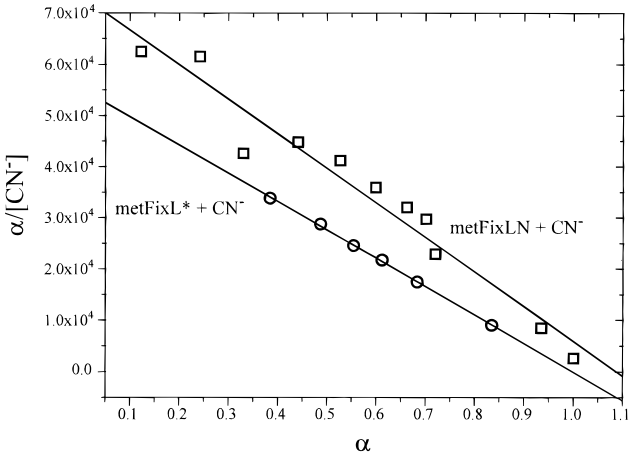

FIGURE 7: Scatchard plots for titration of 1.0 μM metFixLN (squares) and metFixL* (circles) with CN^-, 20 mM Tris, pH 7.8, 22 °C. These plots indicate that both proteins bind 1.00 (= $-y$ intercept/slope = 55 323/55 366) CN^- ion/heme.

Table 4 lists the dissociation constants for metFixLN−CN, metFixL*−CN, metMb−CN, and HRP−CN. The CN^- binding experiments were rather arduous due to long equilibration times after each CN^- addition of the spectrophotometric titrations. When these experiments were carried out under aerobic conditions, the resulting binding curves had a sigmoidal shape reminiscent of those for cooperative hemoglobins. However, when oxygen was excluded from the experiment, the CN^- binding curves for FixLN and FixL* were hyperbolic and yielded linear Scatchard plots. Figure 7 shows representative Scatchard plots for the anaerobic titration of both FixL derivatives with CN^-. The Scatchard plots indicate that CN^- binds noncooperatively with 1 ligand bound/metFixLN or metFixL* molecule.

It was necessary to carry out all CN^- titrations under anaerobic conditions to avoid the slow oxidative degradation of CN^-, the rate of which is competitive with coordination of cyanide to the heme iron at the low CN^- concentrations of early titration points. While neither the mechanism(s) nor the rate constant(s) for oxidative degradation of the CN^- solutions is known, the degradation was verified in aerobic CN^- solutions. Stock CN^- solutions (2 mM) left open to air for 12 h would no longer convert metMb to Mb−CN. This cyanide ion degradation was also observed in the

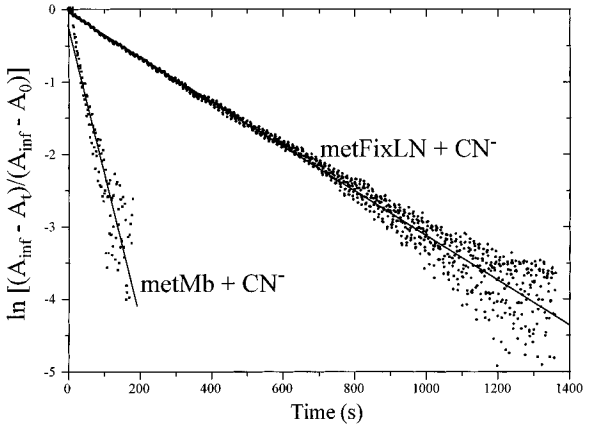

FIGURE 8: Representative first-order plots for the binding of CN^- to metFixLN and metMb under pseudo-first-order conditions. Solution conditions were 1.0 μM protein, 80 μM CN^-, 22 °C, 100 mM Tris, pH 7.8, 5.5% (v/v) glycerol. Rate constants obtained from these data are listed in Table 3.

presence of proteins. If either metMb−CN or metFixL−CN was allowed to sit under aerobic conditions overnight, the UV−visible spectrum of the protein showed that the protein was a mixture of met and met−CN forms. After 48 h, the protein had completely reverted to the met form.

Since these protein−cyanide titrations revealed slow binding of CN^- to metFixLs, the association rate constants were determined for metFixLN−CN and metFixL*−CN under pseudo-first-order conditions. Even though the K_d values of the metFixL−CN adducts and metMb−CN are comparable, the association rate constants for the FixL−CN complexes are significantly smaller that those for metMb and cyanide ion (Table 4). Figure 8 shows this striking difference in association rates for metMb−CN and metFixLN−CN.

The dissociation rate constant for metFixL−CN is an order of magnitude smaller than the k_{off} for metMb−CN. Possible contributors to this diminished k_{off} are (a) an energy barrier to solvation of the dissociated anionic CN^- ligand in the hydrophobic distal heme pocket of FixL and (b) a trans effect of the more protonated imidazole in FixL (Table 2).

A slight but reproducible decrease in the stability of metFixL*−CN relative to that of metFixLN−CN is observed. Table 4 reveals that this decrease is due to a preferential decrease in k_{on} for CN^- binding to metFixL*.

Complexation of metFixLN and metFixL* with the triatomic pseudohalides, azide and thiocyanate ions, was attempted. Neither the azide nor the thiocyanate adducts of FixL could be generated under conditions which facilitate formation of metMb−N_3 or metMb−SCN. Even in the presence of a 10^3-fold excess of ligand, no evidence of the FixL−N_3 or FixL−SCN complexes could be observed at room temperature.

DISCUSSION

The Heme Environment in FixL

The Distal Heme Pocket. Although quantitative interpretation of secondary structure calculations based on CD data tend to be less than straight-forward, the results on oxyFixLN in Figure 2 suggest it is rather unlikely that the heme domain of FixL consists of predominantly α-helical tertiary structure. The presence of some β sheet indicates that the heme pocket may be lined or partially lined by this typically hydrophobic secondary structure. A hydrophobic heme pocket would preclude stabilizing hydrogen-bonding interactions between heme ligands and H-bond donors such as those known to occur in Hb, Mb, and the heme peroxidases [Nakamoto (1980) and references therein]. This is consistent with the diminished O_2 affinity reported for FixL and its various deletion derivatives (Gilles-Gonzalez et al., 1994).

The high core-size marker band frequencies for metFixL relative to aquometMb (Figure 3) indicate that the porphyrin core is less distorted (more planar) in metFixL than in aquometMb. This indicates that the iron atom is further out of the heme plane in metFixL than in the six-coordinate aquometMb (Stryer et al., 1964). Not all of the core-size marker bands (Parthasarathi et al., 1987) conform to this simple model, probably due to differences in the extent of heme doming between the two proteins. The extent of doming in metFixL is probably greater than that in metMb since metFixL is five-coordinate and metMb is six-coordinate. Heme doming is expected to contribute negatively to these frequencies as it distorts the planarity of the heme, thus reducing the skeletal bond strengths, and causes mixing of the in- and out-of-plane vibrational coordinates (Hoard et al., 1973; Spiro et al., 1979; Parthasarathi et al., 1987; Spiro, 1983). Hence, heme core constriction and doming may have opposing effects on the frequencies of some core-size marker bands. The small porphyrin core size of metFixL is consistent with a five-coordinate metFixL heme in which the iron atom is significantly displaced from the mean porphyrin plane. This is consistent with the earlier suggestion that, based on the blue-shifted Soret maximum of metFixL (λ_{max} = 397 nm), it is five-coordinate (Gilles-Gonzalez et al., 1994).

The five-coordinate ferric state of FixL could be the manifestation of distal and/or proximal effects. Proximal tension imposed by the protein might make it difficult to bring the iron close enough to the heme plane for a water molecule to coordinate as a sixth ligand. However, since fluoride ion binds to the heme (Gilles-Gonzalez et al., 1995) to generate a high-spin ferric complex (Table 3), it seems unlikely that H_2O coordination to the ferric heme is precluded by proximal protein conformational tension. Hence, it is concluded that the structural characteristics of the heme pocket responsible for the five-coordinate ferric heme are largely isolated on the distal side of the heme.

The Proximal Heme Pocket. The proximal Fe^{II}−imidazole (Fe^{II}−ImH) stretching vibration (ν_{Fe-ImH}) is typically enhanced in Soret-excited RR spectra of deoxy hemes (Desbois et al., 1981; Spiro, 1985), and the ν_{Fe-ImH} frequency is a sensitive indicator of the Fe^{II}−ImH bond strength. As such, the frequency of this vibration is sensitive to the extent of any H-bonding in which the proximal imidazole may be involved. Donation of the N_1 proton to a H-bonding acceptor imparts partial anionic (imidazolate) character to the proximal histidine, which results in a relatively strong Fe−Im bond. Table 2 lists the ν_{Fe-His} frequencies corresponding to fully protonated imidazoles (top of Table 2) and those deprotonated by H-bond donation to backbone carbonyl groups (middle of Table 2) and to anionic side chains (bottom of Table 2), as occurs in heme peroxidases; *i.e.*, Asp 235 in cyctochrome *c* peroxidase (Poulos & Kraut, 1980; Finzel et al., 1984). The ν_{Fe-ImH} frequency of 212 cm^{-1} in deoxyFixLN and deoxyFixL* falls near the low-frequency end of

the range characteristic of imidazoles that are H-bonded to weak acceptors such as backbone carbonyl groups (Bolton et al., 1970; Ladner et al., 1977). Furthermore, the fact that ν_{Fe-ImH} occurs at the same frequency for both proteins suggests that (a) any interactions between the heme and kinase domains have no measurable effect on the H-bonding status of the proximal imidazole in deoxyFixL and (b) any kinase-based influence on the kinetics or thermodynamics of ligand binding (see below) by the heme most likely arises from adjustment(s) of the distal heme pocket structure.

Response of the Heme Pocket to Interdomain Interactions

Resonance Raman Spectra of FixLN−CO and FixL−CO.* Insight into the effects of interdomain interactions between the heme and kinase domains on the distal heme pocket are provided by Soret-excited RR spectroscopy of the FixLN− and FixL*−CO adducts. The ν_4 vibrational Raman band can be described as the symmetric pyrrole distortion consisting primarily of pyrrole $C_\alpha-N$ and pyrrole $C_\alpha-C_\beta$ stretching and $C_\alpha-C_{meso}$ bending (Li et al., 1990). This band is often referred to as the porphyrin π-electron density marker because it has been shown to reflect the extent of porphyrin π^* population (Spiro & Strekas, 1974; Kitagawa et al., 1975; Spiro & Burke, 1976). In complexes of ferrous hemes with π acidic ligands such as CO and NO, ν_4 shifts to frequencies $\sim$15 cm^{-1} higher than those typical of Fe(II) porphyrins (1350−1355 cm^{-1}). This shift to higher frequency (upshift) is in response to the loss of porphyrin π^* electron density through delocalization into the π^* orbitals of the π-acid ligand (π backbonding). These data are consistent with diminished π backbonding between the Fe(por) moiety and the CO ligand and suggest that the π^* overlap between CO and Fe(por) has been diminished by interaction(s) between the heme and kinase domains. Similar shifts in ν_4 for other heme proteins have been interpreted in terms of a geometrically distorted Fe−C═O moiety (Evangelista-Kirkup et al., 1986; Smulevich et al., 1988). In this model, overlap of the porphyrin and CO π^* orbitals is diminished by off-axis distortion (bending or tilting) of the Fe−C═O unit. This would confine the antibonding electron density to the porphyrin-based π^* orbitals, thereby lowering porphyrin bond orders and downshifting their stretching frequencies.

Recent calculations suggest that the energy cost of an off-axis distortion such as that described above is too large to be imposed by protein conformational strain (Ray et al., 1994). Experimental evidence from the same investigators suggests that perturbations in π backbonding result primarily from distal electrostatic fields that are asymmetric with respect to the C_{4v} axis of the porphine core (Ray et al., 1994). Regardless of the mechanism by which the heme−CO backbonding is perturbed, a distorted Fe−C═O moiety is consistent with differences in the shape and/or electrostatic field in the distal heme pocket between FixLN−CO and FixL*−CO.

Figure 5 reveals that ν_4 for FixL*−CO is slightly more broad (by 1.8 cm^{-1}) than the corresponding band in the FixLN−CO spectrum. This may indicate multiple conformations at the periphery of the heme that arise in response to the asymmetry in the distal pocket that downshifts the ν_4 frequency in FixL*−CO.

^{1}H NMR Spectra of metFixLN and metFixL.* The broad resonance centered near 100 ppm in the metFixL* ^{1}H NMR spectrum (Figure 6) could be due to unresolved peaks in the FixL* spectrum corresponding to protons that are not within the paramagnetic influence of the heme in metFixLN. However, the similarity in the Soret-excited RR spectra of metFixLN and metFixL* suggest that these protons are unlikely to be covalently attached to the heme, which would require a *ca*. 95-ppm downfield dipolar shift of these protons. This is an impossible set of circumstances, as the protons would have to be nearly in the plane of the porphyrin and very close to the heme iron to experience a dipolar shift of this sign and magnitude (La Mar & Walker, 1979). It is, therefore, proposed that the width and slight downfield shift of the 100-ppm methyl resonance seen in Figure 6 reflects multiple conformations of the protein near the affected methyl group due to the heme−kinase interaction in FixL*. Such an asymmetric perturbation of the heme pocket in FixL* is consistent with the differences between ν_4 frequencies and line widths in the RR spectra of FixLN−CO and FixL*−CO in Figure 5.

*Ligand Binding to FixLN and FixL**

Fluoride Binding to metFixLN. The K_d for metFixLN−F (Table 3) are smaller than those for the respective Mb and HRP adducts and the rates of metFixL−F formation are intermediate between the two proteins. The increased rates of association relative to metMb arise from several effects. First, due to the small ionic radius of the fluoride ion, its approach to and bond formation with the heme iron are less affected by the geometric constraints responsible for the shape selectivity of the FixL heme pocket. Second, whereas metMb has a water molecule bound in its distal coordination site, FixL does not. Hence, coordination of F^- to the FixL heme does not require predissociation of water. Finally, the crystal structure of metHb−F contains a water molecule bridging the fluoride and the distal histidine in a H-bonding network (Deatherage et al., 1976). Since the H-bonding networks in Hb and Mb are similar, water likely occupies a similar site in metMb−F. While this effect may be relatively small, the requirement for this ternary arrangement may also contribute to the increased association rate for metFixLN−F over metMb−F. The increased dissociation rate for metFixL−F over its Mb counterpart may also be grounded in its lack of the H-bonding network that stabilizes the bound F^- in the globins (Deatherage et al., 1976).

The stability of HRP−F is considerably lower than that of FixLN−F due to its large k_{off} (Dunford & Alberty, 1967). This is consistent with the difference in charge of the proximal imidazole ligands in FixL and HRP. The N_1 proton of HRP is strongly H-bonded to a proximal anionic amino acid side chain and, consequently, has considerable imidazolate character (Behere et al., 1985; La Mar et al., 1982; Thanabal et al., 1988, Teraoka & Kitagawa, 1980). The imidazolate ligand partially neutralizes the positive charge of the iron center which, in turn, reduces the activation energy for the separation of charge necessary for fluoride dissociation.

The formation of a six-coordinate high-spin metFixLN−F complex begs the question, why does the high-spin ferric heme not coordinate a water molecule? Formation of the fluoride complex is evidence that a six-coordinate high-spin ferric heme complex is possible for FixL. Hence, it is probably not reasonable to conclude that the protein exerts

too much proximal tension holding the heme iron out of the porphyrin plane and out of the range for bond formation with distal ligands. However, the fluoride binding properties of metFixL are consistent with electrostatic and/or steric constraint serving to discriminate against polyatomic ligands based on shape and size.

*Cyanide Binding to metFixLN and metFixL**. The thermodynamic stabilities of metFixLN−CN and metFixL*−CN are comparable to that of metMb−CN (see Table 4). These results differ slightly from the stabilities of metFixL−CN derivatives determined for the soluble metFixL from *Bradyrhizibium japonicum* (*Bj*FixL) and for a heme domain deletion derivative of *R. meliloti* FixL, RmFixLH (Gilles-Gonzalez et al., 1995). These proteins are reported to reach half-saturation at 350 and 35 μM CN^-, respectively. Based on the K_ds in Table 4, half-saturation occurs at 18.0 μM for metFixL* and 14.8 μM for metFixLN. These half-saturating CN^- concentrations are not directly comparable, because CN^- binding to the met*Bj*FixL and met*Rm*FixLH derivatives, has been reported to be cooperative with a Hill coefficient of 1.7 (Gilles-Gonzalez et al., 1995). Although the sequences of these two FixLs are highly homologous, native *Bj*FixL is a soluble protein. Hence, these apparent discrepancies may arise from differences in primary and possibly secondary and tertiary structures of these FixLs from different organisms. On the other hand, if the rate constants for association of CN^- with met*Bj*FixL are similar to those reported herein for met*Rm*FixL derivatives (Table 4), the 10-min equilibration times reported for met*Bj*FixL and met*Rm*FixLH would only be sufficient for large excesses of CN^- over heme. Either competitive CN^- degradation by O_2 at low [CN^-] or insufficient equilibration time would result in apparent cooperativity. Hill coefficients up to 2.5 have been observed and reported for the CN^- binding curves of metMb (Scheler & Jung, 1958). This may be due to the same oxidative CN^- degradation observed in this study. It seems unlikely that a heme protein containing a single heme would bind CN^- cooperatively unless the protein exists as an oligomer or undergoes a [CN^-]-dependent oligomerization reaction. Although there is currently no evidence to suggest such an oligomerization for FixLs, it is not inconceivable in the context of other two-component receptor proteins such as the transmembrane aspartate receptor in the bacterial chemotaxis system. The single-crystal X-ray structure of the ligand-binding domain of this protein suggests that it senses aspartate via an aspartate-dependent dimerization mechanism (Milburn et al., 1991).

It is curious that the affinities of metFixLN and metFixL* for CN^- are so similar to that of metMb in light of the fact that the stabilities of ferrous FixL−O_2 and FixL−CO complexes are considerably lower than those of the analogous Mb complexes (Gilles-Gonzalez et al., 1994). The diminished stabilities of these complexes has been attributed exclusively to a decrease in the association rate constants (k_{on}), as the dissociation rate constants are similar to those for Mb and Hb (Gilles-Gonzalez et al., 1994). In the case of metFixL−CN, both the association *and* dissociation rate constants are diminished roughly 10-fold relative to those for metMb. While CN^- dissociation requires separation of the negative CN^- ion from the trivalent iron center in both metFixL and metMb, there must be an additional kinetic barrier to dissociation in metFixL−CN. The weakly H-bonded (and, consequently, less negatively charged) proximal imidazole of metFixL has less of a neutralization effect on the positive charge on the heme Fe than the more strongly H-bonded (and anionic) proximal imidazole of Mb. Therefore, metFixL−CN is expected to have a larger electrostatic barrier to separation of the anionic CN^- ligand from the trivalent Fe atom than metMb−CN. Furthermore, RR and UV−visible evidence for a five-coordinate ferric heme suggests that the additional energy barrier to metFixL−CN dissociation may be due in part to the lack of available water to solvate the CN^- anion in the hydrophobic heme pocket.

The FixL heme environment presents kinetic (activation) barriers to both CN^- coordination and dissociation that are not found in the reaction of CN^- with aquometMb. Displacement of a water ligand is unnecessary since metFixL is five-coordinate. In light of the rapid association between F^- and FixL, the slow association rate with CN^- is probably due to factors (steric and/or electrostatic) which slow down the approach of CN^- to the heme iron.

It is useful to compare and contrast the rate constants for fluoride and cyanide binding to and dissociation from metFixLN. The k_{on} for F^- is 5.8 times that for CN^-, which is attributed to the small ionic radius of the fluoride ion and its ability to circumvent the steric constraints of the heme pocket. The greatly increased dissociation rate of metFixLN−F over the CN^- adduct is explained in terms of spin state of the Fe(III) center. Fluoride ion, being a weak-field ligand, forms a high-spin complex with the ferric heme. Since high-spin iron(III) is of considerably larger covalent radius than low-spin iron(III) (average HS Fe−N = 2.069 Å, average LS Fe−N = 1.986 Å) (Scheidt & Gouterman, 1983), the energy cost of expanding the rigid porphine core makes it difficult to force the high-spin iron(III) into the heme plane. Hence, it is reasonable to assume that the iron atom in metFixL−F is displaced considerably to the proximal side of the heme. This distance is 0.3 Å in metHb−F, only 0.1 Å closer than in aquometHb (Deatherage, et al., 1976). The large k_{off} value for the F^- complex is thus a consequence of a long and weak Fe^{III}−F bond with a correspondingly low activation barrier to dissociation.

Lack of Reactivity with Thiocyanate and Azide. The ferric forms of Hb, Mb, and several heme peroxidases readily form stable complexes with the SCN^- and/or N_3^- pseudohalide ligands (Antonini & Brunori, 1971). Hence, if these ligands were accommodated in the distal heme pocket of FixL, one would expect them to form stable adducts with the ferric heme in both metFixLN and metFixL*. However, even in the presence of $\geq 10^3$-fold excesses of these ligands, formation of the adducts was not observed under ambient conditions. The inability of metFixLs to bind either of these ligands supports the idea that steric constraint(s) play an important functional role in the distal heme pocket. Specifically, it suggests that, although the formation of these adducts is probably enthalpically favorable, the heme pocket is sufficiently sterically encumbered to preclude binding of the ligand.

The ligand binding properties of metFixLN and metFixL* raise an interesting physiological issue. The unique high-spin five-coordinate state of the ferric heme in metFixL means that the met and deoxy forms of FixL have similar heme geometries due to their equivalent coordination numbers and high-spin states. Hence, it is reasonable to suggest that they also have similar protein conformations. Since FixLs have relatively large rate constants for autoxidation

(Gilles-Gonzalez et al., 1994), the similarity between their met and deoxy forms is of potential importance to the bacterium. Should the cell find itself under conditions of high oxygen concentration, a significant fraction of the FixL receptors could, in principle, be oxidized to the met form. Since metFixL contains a five-coordinate high-spin heme, the kinase in this state of the protein would be *active* in spite of the presence of oxygen. Because the binding of anionic ligands by metFixL is quite slow (this work) on the time scale of O_2 binding (Gilles-Gonzalez et al., 1994) to deoxyFixLs, deactivation of the met form by exogenous ligand binding would be too slow to facilitate effective transcriptional regulation. Hence, it is difficult to see how the cell could tolerate a significant amount of metFixL under aerobic conditions. This suggests that, in spite of the propensity for rapid autoxidation of deoxyFixL *in vitro*, the *Rhizobium* bacteria must have a mechanism by which they are able to maintain their FixL in the oxy form *in vivo*.

Effect of Heme−Kinase Interactions on Formation Rates and Stabilities of Ligand Complexes. The kinetic and thermodynamic differences between FixLN and FixL* seem to result from influence of the kinase domain on ligand approach to the heme iron and steric constraints on the binding geometry inherent to the heme domain itself. The observed differences between the kinetics and thermodynamics of CN^- binding to FixLN and FixL* are consistent with different conformational states of these two proteins. The conformation of the heme-binding domain in FixL* is altered relative to that of FixLN by virtue of the interplay between the heme and kinase domains in FixL*, which is absent in FixLN. Perturbation of the interactions between the heme and kinase domains that results in communication of changes in heme ligation and spin states to the kinase domain likely relies, at least in part, on this conformational interplay in FixL*.

Placement of steric bulk in the vicinity of the heme through interactions with the kinase domain is evidenced by several observations. First, the ^{1}H NMR spectrum of metFixL* shows one anomalously broadened and shifted methyl resonance that is clearly not broadened in the metFixLN spectrum (Figure 6). This breadth is attributed to conformational heterogeneity in the vicinity of one methyl group due to the presence of the kinase domain and its interaction(s) with the heme domain. Second, the difference in the π electron density marker frequencies of metFixLN−CO and metFixL*−CO also indicate an anisotropic perturbation of the heme pocket structure. Third, binding of the triatomic azide and thiocyanate ions to metFixL is not observed, even in the presence of 10^3-fold molar excess of ligand. Since both of these ligands are known to coordinate to ferric hemes in Hb, Mb, and heme peroxidases, the lack of binding in FixL is consistent with steric encumbrance of the ligand binding site that precludes binding of these triatomic pseudohalide ligands. Finally, the association rate constant of CO with a functional heme−kinase, deoxy*Bj*FixL, is smaller than that for the heme domain alone (Gilles-Gonzalez et al., 1994). This is not observed for O_2, suggesting that the FixL* heme pocket kinetically discriminates against ligands containing more than two atoms and against diatomic ligands such as CO and CN^- whose lowest-energy coordination geometries are linear.

A recent and elegant RR study of the CN^- adducts of cytochrome P-450 in its substrate-bound and substrate-free forms reveals both linear and bent conformations of the Fe−CN moiety with its bending and stretching frequencies being sensitive to occupation of the substrate binding site (Simianu & Kincaid, 1995). A similar analysis comparing metFixL−CN with metFixL*−CN is ongoing in this laboratory and will be reported elsewhere.

On the basis of the available spectroscopic and activity data, it seems clear that the purpose of the heme domain is to communicate the level of cellular oxygen tension to the kinase. Two mechanisms can be envisioned for this communication. One is analogous to that for the NO sensor, soluble guanylyl cyclase (sGC), which modulates the catalytic conversion of guanosine 5′-triphosphate (GTP) to 3′,5′-cyclic guanosine monophosphate (cGMP) as a function of NO partial pressure (concentration) (Garber et al., 1994; Stone et al., 1994; Hursman et al., 1995; Burstyn et al., 1995). Initiation of this signal involves breaking of the proximal Fe−ImH bond in response to binding of NO by the heme. The second is more reminiscent of Hb wherein the oxygen binding and iron spin-state conversion are conveyed to neighboring subunits via displacement of the proximal histidine (and, therefore, the F helix) by movement of the low-spin iron into the heme plane (Perutz, 1990). Recent studies also reveal that distal conformational response to heme ligation is also important in communicating the ligation event to neighboring subunits (Rodgers et al., 1992; Rodgers & Spiro, 1994; Jayaraman et al., 1995). The intersubunit communication stems from the propagation of these local conformational adjustments to the subunit interfaces. Since the UV−visible spectra of oxyFixLs and oxyHb are very similar and since even the NO adduct of FixL has its Fe−His bond intact at physiological temperature (Rodgers et al., 1996), it is reasonable to conclude that the Fe−ImH bond in oxyFixL is intact, making the Hb-like mechanism the most likely. We propose that the local conformational tension induced by binding of O_2 is transmitted to one or more interfacial contacts between the heme and kinase where one or more changes in the nature and free energy of the contacts are elicited. These changes may involve the making or breaking of H-bonds and/or salt bridges between the surfaces of the heme and kinase domains. Any such ligation-induced perturbation(s) of the interdomain interface would likely induce a conformational transition in the kinase, thereby inhibiting its activity.

SUMMARY AND CONCLUSIONS

The heme domain of FixL and the local heme environment are unique among heme proteins. The data presented here indicate that the heme pocket is rather hydrophobic and further suggest that ligand approach and coordination geometry are controlled by placement of steric bulk in the distal heme pocket. The CN^--binding data (this work) along with published kinetic and thermodynamic data on O_2 and CO binding (Gilles-Gonzalez et al., 1994) provide compelling evidence that the interactions between the heme and kinase domains diminish both the rate at which these ligands form complexes with the heme and the thermodynamic stability of the complexes. These observations suggest two possibilities, which need not be mutually exclusive. First, conformational control over the interfacial contact(s) may be affected by ligation-induced changes on both the proximal and distal sides of the heme. Second, a feedback mechanism by which the kinase affects control over ligand affinity and

binding kinetics of the heme likely exists. In order for this process to have some physiological relevance, the ligand binding properties of FixL* would have to be sensitive to a kinase-associated parameter such as the state of kinase phosphorylation or the presence of bound ATP or ADP. The effects of these kinase-associated parameters are currently under investigation in our laboratory.

ACKNOWLEDGMENT

We express our gratitude to Professor Donald Helinski for supplying the expression plasmids pGG820 and pEM130. We also thank Professor Eugene Berry in the NDSU Virology Department for providing us open access to his centrifugation facilities. One of us (J.A.B.) would like to thank the Goldwater Foundation for financial support of his work on this project.

REFERENCES

Antonini, E., & Brunori, M. (1971) Hemoglobin and Myoglobin in Their Reactions with Ligands; *Frontiers of Biology*, Vol. 21, North-Holland Publishing Co., Amsterdam.
Batut, J., Daveran-Mingot, M. L., David, M., Jacobs, J., Garnerone, A. M., & Kahn, D. (1989) *EMBO J. 8*, 1279−1286.
Behere, D. V., Gonzalez-Vergara, E., & Goff, H. M. (1985) *Biochim. Biophys. Acta 832*, 319−325.
Blank, J., Graf, W., & Sheler, W. (1961) *Acta Biol. Med. Germ. 7*, 323.
Bolton, W., & Perutz, M. F. (1970) *Nature 228*, 551−552.
Burstyn, J. N., Yu, A. E., Dierks, E. A., Hawkins, B. K., & Dawson, J. H. (1995) *Biochemistry 34*, 5896−5903.
David, M., Daveran, D. M., Batut, J., Dedieu, A., Domergue, O., Gai, J., Hertig, C., Boistard, P., & Kahn, D. (1988) *Cell 54*, 671−683.
Dawson, J. H., & Sono, M. (1987) *Chem. Rev. 87*, 1255.
Deatherage, J. F., Loe, R. S., & Moffat, K. (1976) *J. Mol. Biol. 104*, 723−728.
Deinum, G., Stone, J. R., Babcock, G. T., & Marletta, M. A. (1996) *Biochemistry 35*, 1540−1547.
Ditta, G., Virts, E., Palomares, A., & Kim, C. H. (1987) *J. Bacteriol. 169*, 3217−3223.
Dunford, H. B., & Alberty, R. A. (1967) *Biochemistry 6*, 447−451.
Dunford, H. B. (1986) in *Advances in Inorganic and Bioinorganic Mechanisms* (Sykes, A. G., Ed.) Vol. 4, pp 41−68, Academic Press, London.
Earl, C. D., Ronson, C. W., & Ausubel, F. M. (1987) *J. Bacteriol. 169*, 1127−1136.
Ellis, W. D., & Dunford, H. B. (1968) *Biochemistry 7*, 2054−2062.
Evangelista-Kirkup, R., Smulevich, G., & Spiro, T. G. (1986) *Biochemistry 25*, 4420−4425.
Finzel, B. C., Poulos, T. L., & Kraut, J. (1984) *J. Biol. Chem. 259*, 13027−13036.
Garber, D. L., & Lowe, D. G. (1994) *J. Biol. Chem. 269*, 30741−30744.
Gilles-Gonzalez, M. A., Ditta, G. S., & Helinski, D. R. (1991) *Nature 350*, 170−172.
Gilles-Gonzalez, M. A., Gonzalez, G., Perutz, M. F., Kiger, L., Marden, M. C., & Poyart, C. (1994) *Biochemistry 33*, 8067−8073.
Gilles-Gonzalez, M. A., Gonzalez, G., & Perutz, M. P. (1995) *Biochemistry 34*, 232−236.
Goff, H. M. (1982) in *Iron Porphyrins—Part I* (Lever, A. B. P., & Gray, H. B., Eds.) pp 237−281, Addison-Wesley, Reading, MA.
Ho, C. (1992) *Adv. Protein Chem. 43*, 153−312.
Hursman, A. R., & Marletta, M. A. (1995) *Biochemistry 33*, 5627−5634.
Jayaraman, V., Rodgers, K. R., Mukerji, I., & Spiro, T. G. (1995) *Science 269*, 1843−1848.
Kitagawa, T., Iizuka, T., Saito, M., & Kyogoku, Y. (1975) *Chem. Lett.*, 849.
Kitagawa, T., Nagai, K., & Tsubaki, M. (1979) *FEBS Lett. 104*, 376−378.
Ladner, R. C., Heidner, E. J., & Perutz, M. F. (1977) *J. Mol. Biol. 114*, 385−414.
La Mar, G. N., & Walker, F. A. (1979) in *The Porphyrins* (Dolphin, D., Ed.) Vol. IV, Chapt. 2, pp 61−157, Academic Press, New York.
La Mar, G. N., Budd, D. L., Smith, K. M., & Langry, K. C. (1980) *J. Am. Chem. Soc. 102*, 1822−1827.
La Mar, G. N., De Ropp, J. S., Chacko, V. P., Satterlee, J. D., & Erman, J. E. (1982) *Biochim. Biophys. Acta 708*, 317−325.
Li, X.-Y., Czernuszewicz, R. S., Kincaid, J. R., Stein, P., & Spiro, T. G. (1990) *J. Phys. Chem. 94*, 47−61.
Lukat, G. S., Rodgers, K. R., Jabro, M. N., & Goff, H. M. (1989) *Biochemistry 28*, 3338−3344.
Milburn, M. V., Prive, G. G., Milligan, D. L., Scott, W. G., Yeh, J., Jancarik, J., & Koshland, D. E., Jr. (1991) *Science 254*, 1342−1347.
Monson, E. K., Weinstein, M., Ditta, G. S., & Helinski, D. R. (1992) *Proc. Natl. Acad. Sci. U.S.A. 89*, 4280−4284.
Monson, E. K., Ditta, G. S., & Helinski, D. R. (1995) *J. Biol. Chem. 270*, 5243−5250.
Nagai, K., & Kitagawa, T. (1980) *Proc. Natl. Acad. Sci. U.S.A. 77*, 2033−2037.
Nakamoto, K. (1990) *Coord. Chem. Rev. 112*, 363−402.
Parthasarathi, N., Hanson, C., Yamaguchi, S., & Spiro, T. G. (1987) *J. Am. Chem. Soc. 109*, 3865.
Perutz, M. F. (1990) *Annu. Rev. Physiol. 52*, 1−25.
Poulos, T. L., & Kraut, J. (1980) *J. Biol. Chem. 255*, 8199−8205.
Ray, G. B., Li, X.-Y., Ibers, J. A., Sessler, J. L., & Spiro, T. G. (1994) *J. Am. Chem. Soc. 116*, 162−176.
Reyrat, J., David, M., Blonski, C., Boistard, P., & Batut, J. (1993) *J. Bacteriol. 175*, 6867−6872.
Rodgers, K. R., & Spiro, T. G. (1994) *Science 265*, 1697−1699.
Rodgers, K. R., Su, C., Subramaniam, S., & Spiro, T. G. (1992) *J. Am. Chem. Soc. 114*, 3697−3709.
Rodgers, K. R., Lukat-Rodgers, G. S., & Barron, J. A. (1996) *J. Am. Chem. Soc.* (submitted for publication).
Scheidt, W. R., & Gouterman, M. (1982) in *Iron Porphyrins—Part I* (Lever, A. B. P., & Gray, H. B., Eds.) pp 89−140, Addison-Wesley, Reading, MA.
Scheler, W., & Jung, F. (1958) *Acta Biol. Med. Germ. 1*, 232.
Simianu, M. C., & Kincaid, J. R. (1995) *J. Am. Chem. Soc. 117*, 4628−4636.
Spiro, T. G. (1983) in *Iron Porphyrins—Part II* (Lever, A. B. P., & Gray, H. B., Eds.) pp 89−159, Addison-Wesley, Reading, MA.
Spiro, T. G. (1985) in *Advances in Protein Chemistry*, Vol. 37, pp 111−159, Academic Press, New York.
Spiro, T. G., & Strekas, T. C. (1974) *J. Am. Chem. Soc. 96*, 338.
Spiro, T. G., & Burke, J. M. (1976) *J. Am. Chem. Soc. 98*, 5482.
Spiro, T. G., Stong, J. D., & Stein, P. (1979) *J. Am. Chem. Soc. 101*, 2648−2655.
Smulevich, G., Mauro, J. M., Fishel, L. A., English, A. M., Kraut, J., & Spiro, T. G. (1988) *Biochemistry 27*, 5486−5492.
Smulevich, G., Hu, S., Rodgers, K. R., Goodin, D. B., Smith, K. M., & Spiro, T. G. (1996) *Biospectroscopy* (in press).
Sreerama, N., & Woody, R. W. (1993) *Anal. Biochem. 209*, 32−44.
Stone, J. R., & Marletta, M. A. (1994) *Biochemistry 33*, 5636−5640.
Stryer, L., Kendrew, J. C., & Watson, H. C. (1964) *J. Mol. Biol. 8*, 96.
Teraoka, J., & Kitagawa, T. (1980) *J. Phys. Chem. 84*, 1928−1935.
Teraoka, J., & Kitagawa, T. (1981) *J. Biol. Chem. 256*, 3969−3977.
Thanabal, V., de Ropp, J. S., & La Mar, G. N. (1988) *J. Am. Chem. Soc. 110*, 3027−3035.

BI9530853